

## Computer simulations on the cyclic deformation of a single polymer chain above and below the $\Theta$ temperature

Stefan Kreitmeier, Markus Wittkop, and Dietmar Göritz

*Institut für Experimentelle und Angewandte Physik, Universität Regensburg, D-93040 Regensburg, Germany*

(Received 3 August 1998)

The cyclic deformation behavior of a single three-dimensional polymer chain above and below the  $\Theta$  temperature was studied using the bond-fluctuation model. Whereas above  $T_\Theta$  the entropy controls the deformation, below  $T_\Theta$  a completely changed behavior was found. Due to the dominating energetic part a globule-strand system is generated. A comparison with a theoretical concept of Halperin and Zhulina is presented. A reasonable description is possible, however, some deviations remain. A discussion on the necessary relaxation time or complimentary the drawing velocity is given. An Arrhenius-type-like dependency was found which considerably lengthens any simulation of cold polymer systems. [S1063-651X(99)03202-X]

PACS number(s): 36.20.Ey, 87.15.-v, 83.20.Jp

### I. INTRODUCTION

The mechanical properties and deformation behavior of polymers have attracted much attention in polymer physics. Therefore much work has been undertaken to understand the microscopic mechanisms of the deformation process. Of special interest in recent times is the investigation of biopolymers such as DNA and titin [1–6] in their stretching and unfolding behavior. Sophisticated tools such as optical tweezers or modified atomic force microscopes for force length detections were taken. Stress-strain relations were measured and discussed in the framework of wormlike chains. Some experiments, however, for example, on titin [4], show a plateau regime within the stress-strain curves, which cannot be explained by standard deformation theories. Thus, up to now it has been rather difficult to obtain complete and fully conclusive results regarding microscopic details of deformation processes from experiments, although promising first steps have been done.

From a theoretical point of view different regimes can be distinguished. In the athermal limit with purely excluded volume interactions a linear force regime and a regime with Pincus scaling [7] can be distinguished [8–10]. These regimes and the crossover region between them have been well investigated [11–13] and can be described by scaling functions obtained from renormalization group studies. A comparison with Monte Carlo simulations can be found, for example, in Refs. [14,15]. With decreasing temperature the attractive interactions start to dominate. Hence at low temperatures the chain collapses into a compact dense globule. At an intermediate temperature, the  $\Theta$  temperature  $T_\Theta$ , the repulsive and attractive parts of the interaction cancel each other [16]. The deformation behavior below the  $\Theta$  temperature is expected to be completely different from that above  $T_\Theta$ . A constancy of the force was proposed in the coil-strand-transition model [17,18]. Within a blob concept Halperin and Zhulina [19] calculated a constant force regime which involves a coexistence of a weakly deformed globule and a highly stretched strand.

To check these predictions in the above described experimental situation computer simulations are a simple and reli-

able method. Recently, results on the loading process of single chains at low temperatures have been obtained in computer simulations [20–24]. A bimodal shape of the end-to-end vector distribution function of stretched chains seems to indicate a coexistence of molecules in globular and extended coil formations [20,21]. In conformational plots and stress-strain studies we were able to confirm the formation of a globule-strand system [22–24].

Despite all these efforts, the exact processes during the formation and disintegration of a globule-strand system still need further investigation. Moreover no data exists on the unloading part of the deformation below  $T_\Theta$ . Hence the intention of this paper is to perform computer simulations in order to analyze the changes of the total force with respect to its energetic and entropic contributions during the cyclic deformation. A comparison with the theory of Halperin and Zhulina will be given.

### II. THEORETICAL

As we would like to compare our results to the prediction of Halperin and Zhulina we briefly describe their theoretical derivations. Below the  $\Theta$ -temperature  $T_\Theta$  a globule of  $N$  monomers is considered to consist of blobs of size

$$\xi_c = g_c^{1/2} b, \quad (1)$$

$b$  being the monomer length.  $g_c$ , the number of monomers in each blob, can be calculated from

$$g_c \approx \left( \frac{T_\Theta}{\Delta T} \right)^2. \quad (2)$$

$\Delta T = T_\Theta - T$  is the difference in temperature with respect to the  $\Theta$  temperature. The volume of the globule can be obtained by multiplying the number of blobs with the volume of a blob, roughly,

$$V_c \approx \left( \frac{N}{g_c} \right) \xi_c^3. \quad (3)$$

This leads to a radius of the globule  $r_c$  of

$$r_c \approx N^{1/3} \left( \frac{T_\Theta}{\Delta T} \right)^{1/3} b. \quad (4)$$

Let  $\gamma$  be the surface tension between the globule and the solvent. Halperin and Zhulina proposed

$$\gamma = \frac{k_B T}{\xi_c^2}. \quad (5)$$

A minimization of the surface area for different elongations yields the force-elongation relationship

$$\frac{f_0}{k_B T} \approx - \frac{\gamma}{k_B T} (L - r_c) \quad (6)$$

for moderately small deformations ( $L$  current length of the globule). Hence, a linear increase with elongation is found in this regime. For intermediate elongations the result is

$$\frac{f_0}{k_B T} \approx - \frac{\gamma}{k_B T} V_c^{1/2} L^{-1/2}. \quad (7)$$

In further elongation a Pincus [7] behavior is supposed. The relationship for intermediate elongations by imposed elongation shows an instability which is resolved by means of a Maxwell equal-area construction leading to a constant force-elongation relationship

$$\frac{f_0}{k_B T} = - \frac{1}{\xi_c}. \quad (8)$$

The range of validity of this regime is given by

$$\left( \frac{N}{g_c} \right) + 1 < \frac{L}{\xi_c} < \frac{N}{g_c}. \quad (9)$$

The inclusion of finite size effects ultimately leads to

$$f := \frac{f_0}{k_B T} = - \frac{1}{\xi_c} + \frac{1}{r_g} \quad (10)$$

with

$$r_g = (N - N_s)^{1/3} g_c^{-1/3} \xi_c \quad (11)$$

the radius of the momentary globule.  $N_s$  is the number of momomers within the strand. For further information see Ref. [19].

### III. MODEL DESCRIPTION

For the simulations we used the well-known three-dimensional bond-fluctuation model [25,26] with a Van der Waals potential and a suitable bond-length potential. In this coarse-grained lattice model the polymer chains are created by self-avoiding walks on a cubic lattice each monomer occupying eight corners of the unit cell. For more details on the bond-fluctuation model see Refs. [25,26].

#### A. Interactions

Additionally to the purely excluded volume interaction of the bond-fluctuation algorithm a truncated Lennard-Jones

potential  $V(r)$  with a range of three grid units between all points of the monomers ( $r$  is the distance between the monomers) and a bond-length potential  $V'(\ell)$  describing the increasing backbone stiffness with decreasing temperature was taken into account:

$$V(r) = \frac{\epsilon}{2} \left[ \left( \frac{r}{r_0} \right)^{-12} - 2 \left( \frac{r}{r_0} \right)^{-6} \right], \quad (12)$$

$$V'(\ell) = \frac{\epsilon}{2} \left[ c_0 + c_1 \frac{\ell}{a} + c_2 \left( \frac{\ell}{a} \right)^2 + c_3 \left( \frac{\ell}{a} \right)^3 \right], \quad (13)$$

with  $\epsilon$  a unit of energy,  $r_0 = 1.1a$ ,  $\ell$  the bond length, and  $a$  the lattice spacing. The parameters  $c_0 = -207.12$ ,  $c_1 = 342.88$ ,  $c_2 = -163.52$ ,  $c_3 = 24.32$  were estimated from a static energy-minimization simulation, including ten unified PE monomers interacting by bond-stretching, torsional, and Van der Waals forces. The identification of a bond with a Kuhnian segment [27] of ten PE segments is somewhat arbitrary, but is in agreement with values used in the literature [28,29]. With this choice of parameters the chains are flexible in contrast to stiff chains, see Ref. [30]. At low temperatures long bonds are more likely leading to a higher acceptance rate within our model.

#### B. Force determination

According to the following derivations the retractive force, normalized by the temperature,  $f = f_0/k_B T$  ( $k_B$  denotes Boltzmann's constant and  $T$  the temperature) was measured by counting the tried jumps  $n_+$  with  $R_f \rightarrow R_f + a$  and  $n_-$  with  $R_f \rightarrow R_f - a$ . Starting from the total differential of the free energy  $F$  the force  $f_0$  can be obtained by a derivation

$$dF = f_0 dR - p dV - S dT \Rightarrow f_0 = \left( \frac{\partial F}{\partial R} \right)_{T,V}. \quad (14)$$

$F$  is given by

$$F(R) = - \frac{1}{\beta} \ln Z(R) = - \frac{1}{\beta} \ln P(R) + \text{const}. \quad (15)$$

$Z$  is the partition function and  $P(R)$  the probability distribution of the chain end-to-end vector. Hence, approximating the differentiation by the differential quotient

$$f_0 \approx - \frac{1}{a\beta} [\ln P(R) - \ln P(R-a)] \quad (16)$$

and

$$f = \beta f_0 \approx \frac{1}{a} \ln \frac{P(R-a)}{P(R)}. \quad (17)$$

With the assumption of detailed balance

$$P(R)W(R \rightarrow R-a) = P(R-a)W(R-a \rightarrow R), \quad (18)$$

$W$  being the transition probabilities, the equation reduces to

$$f \approx \frac{1}{a} \ln \frac{W(R \rightarrow R-a)}{W(R-a \rightarrow R)}. \quad (19)$$

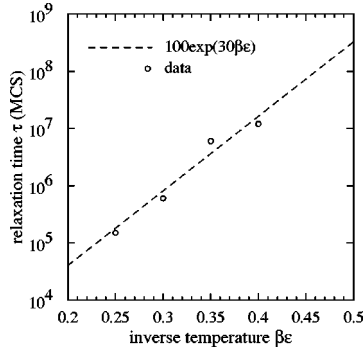


FIG. 1. Relaxation time, necessary for equilibrium deformation, versus  $\beta\epsilon$ . The circles indicate the obtained data. The dashed line is an Arrhenius fit.

Assuming  $W(R-a \rightarrow R) \approx W(R \rightarrow R+a)$  finally leads to

$$f \approx -\frac{1}{a} \ln \frac{W(R \rightarrow R-a)}{W(R \rightarrow R+a)}. \quad (20)$$

The corresponding  $W$  can be calculated through the attempted jumps  $n_-$ ,  $n_+$ .

The energetic part of the force  $\langle f_E \rangle$  was determined from the energy  $\langle E \rangle$  of the chain according to  $\langle f_E \rangle = \beta(d\langle E \rangle/dR_f)$ ,  $\beta = 1/k_B T$  being the inverse temperature. Unfortunately a distinction between surface energy and bulk energy was not possible. With  $\langle f_E \rangle$  and the total force  $\langle f \rangle$ , it is straightforward to evaluate the entropic part of the force  $\langle f_S \rangle$  by  $\langle f_S \rangle = \langle f \rangle - \langle f_E \rangle$ .

### C. Deformation procedure

The deformation was imposed by stepwise changes of the end-to-end distance  $R_f$  in the  $z$  direction. After each deformation step a relaxation to the equilibrium was performed. To ensure equilibrium conditions the proper relaxation time after each deformation step must be found. This was reached by the following procedure: each sample was stretched with fixed relaxation time of 150 000 MCS to an elongation of about  $25a$ . (1 MCS, one Monte Carlo step, is one attempted jump per monomer.) The system was kept at this elongation and permitted to relax. The changes in the force were recorded until steady state was achieved. From this procedure the relaxation time  $\tau$ , displayed in Fig. 1 vs inverse temperature, was obtained.

A complete deformation cycle was then carried out as follows: First  $R_f=0$  was assured. Since no constraints in the  $x$  and  $y$  direction are present  $R_f=0$  permits  $f=0$ . After a relaxation with fixed ends the distance  $R_f$  was increased stepwise by an amount of  $2a$ . After each deformation step an equilibration run was carried out with relaxation time  $\tau$  as obtained in the above described preceding experiments. A deformation velocity may be defined by  $2a/\tau$ . Then the measurements of the momentary force and energy were performed. The unloading process was simulated by decreasing  $R_f$  in the same manner. A complete discussion of the non-equilibrium effects during a cyclic experiment will be given in a forthcoming paper.

In the present simulation we studied single chains consisting of 60 monomers. To obtain proper statistics we performed 100 independent simulations.

## IV. RESULTS AND DISCUSSION

In our simulation model the  $\Theta$  temperature is given by  $\beta_\Theta \epsilon = \epsilon/(k_B T_\Theta) = 0.214 \pm 0.008$  shown in detail in another paper [31]. The different results for the deformation behavior above and below  $T_\Theta$  can be seen in Fig. 2. In this figure the total force  $\langle f \rangle$  (solid lines), the energetic part  $\langle f_E \rangle$  (dashed lines), and the entropic part  $\langle f_S \rangle$  (dashed-dotted lines) are plotted versus the strain  $R_f$ . The arrows indicate the loading or unloading process. A conformational description of the cyclic deformation in the case  $T < T_\Theta$  is displayed in Fig. 3. It should be stated that the discussed cyclic behavior does not depend on the special cycle under consideration. This was checked by simulating more than one cyclic deformation of the same sample.

### A. Above the collapse temperature

Above  $T_\Theta$  at  $\beta\epsilon=0.1$  and  $\beta\epsilon=0.2$  [Figs. 2(a), 2(b)] the energetic part of the force  $\langle f_E \rangle$  nearly vanishes. Hence the total force is almost identical to the entropic part of the force. The deformation is obviously controlled by the entropy. In a study of the conformational changes [23] it could be seen that at temperatures above  $T_\Theta$  an affine deformation of the random coil takes place. Thus, the deformation is homogeneous. The behavior of the total force is very similar to that at  $\beta\epsilon=0$ . As discussed in Ref. [14] in the athermal case  $\beta\epsilon=0$  the curve of  $\langle f \rangle$  can be described for small strains by a linear response to the deformation, i.e.,  $\langle f \rangle = 3R_f/\langle R_N^2 \rangle$  where  $\langle R_N^2 \rangle$  is the mean square end-to-end distance of the undeformed chain. For intermediate strains the force scales with  $R_f$  as  $\langle f \rangle \sim R_f^{3/2}$  [7].

### B. Below the collapse temperature

Below the  $\Theta$  temperature marked changes in the energetic and entropic part of the force occur in the loading and unloading process [Figs. 2(d)–2(f)]. The undeformed chain is in its collapsed state. Starting the elongation the globule is getting stretched to some extent. A more or less linear increase of the force describes this part. Afterwards a plateau regime in the total force can be observed. A strand is torn out of the globule. At midrange elongation ( $R_f \approx 40a - 70a$ , depending on the temperature) the deformation changes back to the behavior above  $T_\Theta$ . The globule-strand system is disintegrating and the chain behaves similar to an affine coil. This disintegration is understandable when using the stability criterion  $(T_\Theta - T) > T_\Theta/N_r^{1/2}$  for globules of chain length  $N_r$  [16,33]. As the number of segments  $N_r$  in the rest globule is decreasing with increasing  $R_f$  the rest globule and therefore the globule-strand system must get unstable for a given temperature  $T$ .

Let us now discuss the implication of the above stated ideas on the energetic and entropic parts of the force. As long as the globule exists the energetic part is strongly retractive and controls the deformation. A segment leaving the globule loses most of its energy gained by the Van der Waals interaction within the globule. (An intermediate step of the mono-

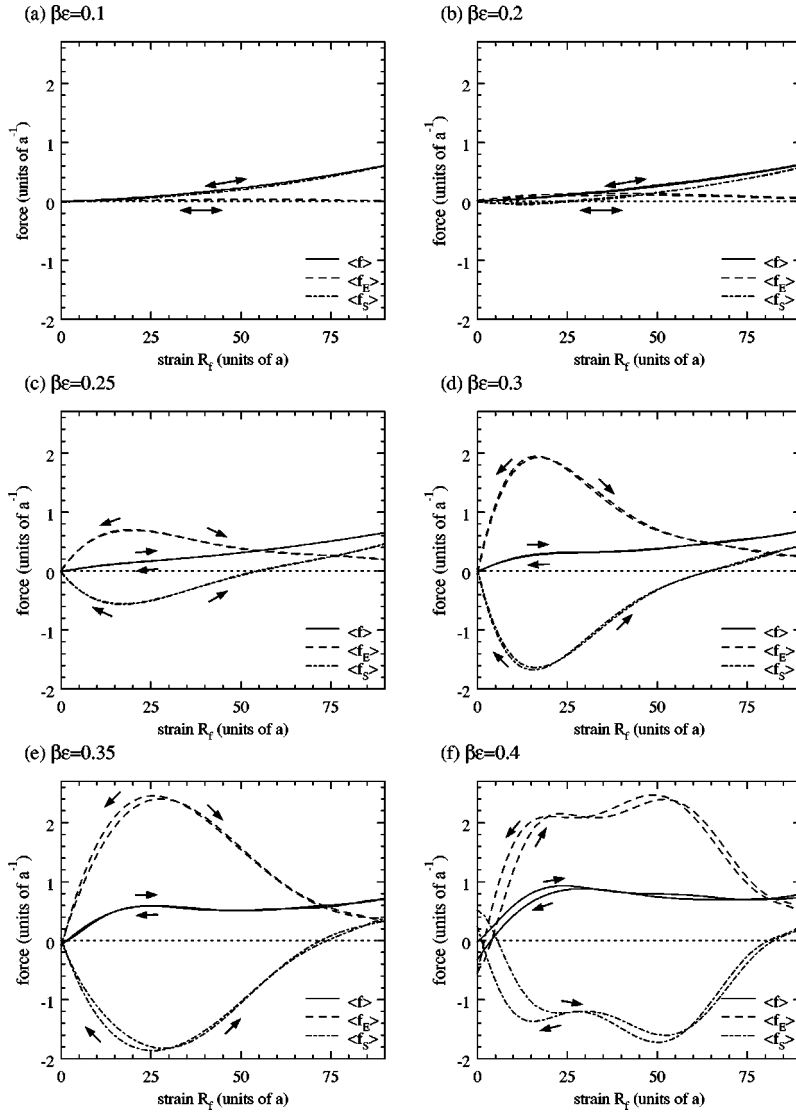


FIG. 2. Total force  $\langle f \rangle$ , energetic part  $\langle f_E \rangle$ , and entropic part  $\langle f_S \rangle$  versus strain  $R_f$ : (a)  $\beta\epsilon=0.1$ , (b)  $\beta\epsilon=0.3$ , (c)  $\beta\epsilon=0.4$ . The arrows indicate the loading or unloading process.

mer of being at the surface will not change this discussion.) This is unfavorable, leading to  $\langle f_E \rangle > 0$ . In contrast, the entropy tries to destroy the globule. The entropy content per segment in the globule is much less than the portion in the formed strand as long as the strand is not too highly oriented, leading to  $\langle f_S \rangle < 0$ . Consequently the entropy tends to transform the globule-strand system into a further stretched but affine strand. When the globule-strand system disintegrates ( $R_f \approx 40a - 70a$ ) the entropic part of the force is rapidly starting to get positive delivering most of the total retractive force as in the case  $T > T_\Theta$ . Again the deformation is controlled by the entropy.

In unloading the same features can be seen just in the opposite direction. First the entropy controls the process. With increasing tendency for collapsing the energetic part is gaining influence. Fluctuating but aligned segments start to diminish the internal energy serving as germination points for the formation of small globules which, in most cases, readily transform into one large globule. A new globule-strand system is created (see Fig. 3, lower part). The small deviations in Fig. 2(f) between loading and unloading hint at

a slight tendency to nonequilibrium effects at that low temperature. However, this should not be taken too seriously.

### C. Comparison to the theory of Halperin and Zhulina

In this section we will try to compare our simulation results to the above described theoretical concepts. We focus on two aspects, namely, the range of validity of the plateau regime and the ratio of the forces in the plateau regime. Taking the Eq. (9) ranges of

$$9.4 < \frac{L}{b} < 17.2 \quad \text{for} \quad \beta\epsilon = 0.3, \quad (21)$$

$$7.9 < \frac{L}{b} < 23.3 \quad \text{for} \quad \beta\epsilon = 0.35, \quad (22)$$

$$7.2 < \frac{L}{b} < 27.9 \quad \text{for} \quad \beta\epsilon = 0.4, \quad (23)$$

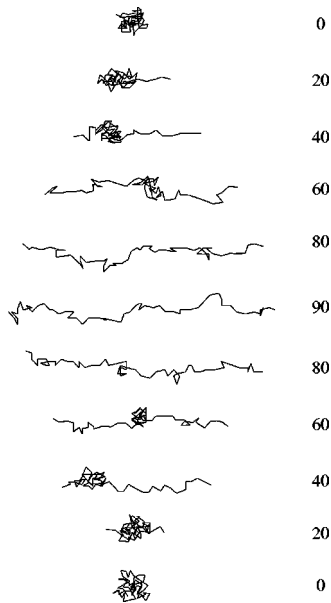


FIG. 3. Snapshot of the conformation of a coil consisting of 60 monomers at different stretching steps  $R_f/a$  during loading and unloading as indicated in the plot. The inverse temperature is  $\beta\epsilon = 0.4$ .

can be calculated. In these inequalities the elongation  $L$  is normalized to the monomer length  $b$ . As our mean bond length is about  $2.7a$  ( $a$  lattice spacing) we should find in our simulations validity ranges of

$$25 < R_f < 46 \quad \text{for } \beta\epsilon = 0.3, \quad (24)$$

$$21 < R_f < 63 \quad \text{for } \beta\epsilon = 0.35, \quad (25)$$

$$20 < R_f < 75 \quad \text{for } \beta\epsilon = 0.4, \quad (26)$$

$R_f$  being our elongation of the deformed chain in lattice spacings. When looking at Figs. 2(d)–2(f) we see good agreement.

The comparison of theoretical force calculations and simulated forces and, hence, a determination of the influence of the surface energy, is somewhat harder to perform. In the theory many  $\approx$  signs hint at some constant factors which should be included for a quantitative description. On the other hand, the potentials used in our simulations will certainly have some influence on the value of the plateau regime. A possible way to cope with these difficulties is to calculate ratios for different temperatures and to hope for a cancellation of these unknown factors. Hence, we evaluated the following ratios:

$$\left| \frac{f_{0.4}}{f_{0.35}} \right|, \quad \left| \frac{f_{0.4}}{f_{0.3}} \right| \quad (27)$$

using Eq. (10) to calculate the single quantities. The indices indicate the corresponding inverse temperatures. In Table I the different parts of the forces determined computer experimentally and theoretically are listed. To include the finite size effect we set  $N_s$  in Eq. (11) to approximately 10. The forces themselves differ considerably when comparing the experimental and theoretical values (Table I), thus confirm-

TABLE I. Values for the force in the plateau regime. Theoretical:  $f_{\text{theo}}/k_B T$  according to Eq. 10 from  $\xi_c$  and  $r_g$ , experimental:  $f_{\text{sim}}/k_B T$  from Fig. 2.

$\beta\epsilon$	$\frac{1}{\xi_c}$	$\frac{1}{r_g}$	$f_{\text{theo}}/k_B T [1/b]$	$f_{\text{sim}}/k_B T [1/a]$
0.25	0.144	0.142	0.002	0.12
0.30	0.286	0.179	0.107	0.28
0.35	0.388	0.198	0.190	0.55
0.40	0.465	0.210	0.255	0.90

ing the above statements on the approximations. The ratios, however, are much closer together.

$$\left| \frac{f_{0.4}}{f_{0.35}} \right|_{\text{theo}} = 1.40 \leftrightarrow \left| \frac{f_{0.4}}{f_{0.35}} \right|_{\text{exp}} = 1.63, \quad (28)$$

$$\left| \frac{f_{0.4}}{f_{0.3}} \right|_{\text{theo}} = 2.38 \leftrightarrow \left| \frac{f_{0.4}}{f_{0.3}} \right|_{\text{exp}} = 3.11. \quad (29)$$

The tendency seems to be qualitatively correct especially when taking into account an error of about 5 to 10 % in the simulated ratios. But whether the deviations are due to additional effects within the globule strand formation or due to an inaccurate inclusion of finite size effects cannot be conclusively judged. The finite size effect for  $\beta\epsilon = 0.25$ , a temperature only slightly below the  $\Theta$  temperature, leads to an almost vanishing force. This should indicate an upper limit for reasonable  $N_s$  values in the range of 10. Taking smaller  $N_s$  values would increase the deviations whereas higher values would lower them.

Calculating the number of monomers per blob  $g_c$  for the different temperatures results in  $g_c \approx 4$  for  $\beta\epsilon = 0.4$ ,  $g_c \approx 6$  for  $\beta\epsilon = 0.35$ ,  $g_c \approx 11$  for  $\beta\epsilon = 0.3$ , and  $g_c \approx 48$  for  $\beta\epsilon = 0.25$ . As the chain length is 60 monomers this, too, shows the influence of the finite size. Around the  $\Theta$  temperature the numbers for one blob and for the assumed strand equals the chain length fairly well. This clearly is a limiting case for any theory using blobs as fundamental units. Hence, some deviations can be expected. At low temperatures about 10 to 15 blobs can be formed within the chain and an applicability of the theory of Halperin and Zhulina to a first approximation should be possible.

#### D. Relaxation times

To discuss the results for the relaxation time  $\tau$  necessary for the equilibrium deformation (see Fig. 1) we compare the results with a characteristic relaxation time  $\tau_1$  derived from the squared displacement of the middle monomers  $g_1(t)$  in the undeformed state

$$g_1(t) = \frac{1}{5} \sum_{i=N/2-2}^{N/2+2} \langle [\vec{r}_i(t) - \vec{r}_i(0)]^2 \rangle. \quad (30)$$

To determine the characteristic relaxation time  $\tau_1$ , we followed the definition by Milchev [32],  $g_1(\tau_1) \equiv \langle S_N^2 \rangle$ ,  $\langle S_N^2 \rangle$  being the averaged radius of gyration. Thus,  $\tau_1$  measures the time needed for a monomer to move a distance in the order

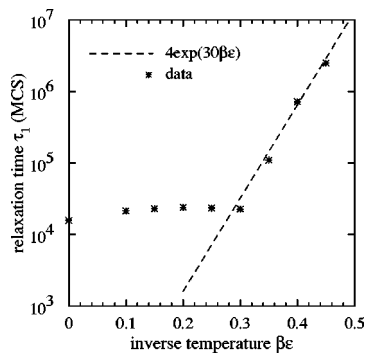


FIG. 4. Relaxation time  $\tau_1$ , obtained from Eq. (30), versus  $\beta\epsilon$ . The stars indicate the obtained data. The dashed line is an Arrhenius fit.

of magnitude of the radius of gyration. Figure 4 displays the results. (More details on the dimensions of the collapsed coils can be found in Ref. [31].) Below  $T_\Theta$  we performed an Arrhenius fit for both relaxation times. The results are shown as the dashed lines in the corresponding figures. In both cases the same activation energy of about  $30\epsilon$  is found. Only the prefactor is different. Roughly spoken,  $\tau$  is approximately  $25\tau_1$ . This result is of twofold interest. Firstly, it shows a clear connection of relaxation processes in the undeformed state with relaxation processes necessary in deforming this system. Secondly, this almost exact relationship between these two in a completely different way obtained relaxation times enhances the confidence in the results of the used simulation technique. (By the way this result confirms nicely the application of the criterion of Milchev to obtain information on the relaxation processes within a polymer system. Only a relatively large prefactor might be necessary for a quantitative description. However, for other simulations of cold systems this increased relaxation time should be taken into account.)

We interpret the result according to the following line. As the temperature dependence is the “same,” the equilibrium deformation is depending on an equilibration of the rest globule. The existence of the strand has obviously no influence on the equilibration process. The strand seemingly attains its equilibrium state much faster. The time dependence

of the deformation is thus solely due to the “bulk” properties of the globule. The activation energy of  $30\epsilon$  is about 3 to 4 times the value gained by one monomer in the globule through the Van der Waals interaction [24]. Thus, the obtained activation energy indicates cooperative processes for movements in the globule.

### E. Implications for biopolymers

Finally we would like to discuss some implications of the above simulations on the investigation of biopolymers. In some respect the deformation of, for example, titin in the initial state resembles a globule-strand transition. The folded protein can be visualized as a collapsed chain. The interior of the folded protein is hydrophobic and, hence, experiences bad solvent conditions. The process of stretching or unfolding can be interpreted as certain segments leaving the initial globule. A strand is formed. According to the computer simulations this leads to a plateau in the stress-strain relationship which nicely corresponds to the experimental findings [4]. Thus, the obtained results from the simulations could have even wider applications, not just for polymers. However, proteins are complex systems compared to simple polymer chains. Therefore some caution has to be taken when interpreting the stress-strain relationships for biopolymers with respect to the upper model system.

### V. CONCLUSION

We presented a computer simulation concerning the deformation of single polymer chains above and below the  $\Theta$  temperature. An interesting globule-strand formation was found for temperatures well below  $T_\Theta$ . The separation of the total force into energetic and entropic parts revealed complex interrelations. A comparison to the theory of Halperin and Zhulina yielded some agreement. However, deviations remain. The time needed to perform equilibrium deformations below  $T_\Theta$  is of Arrhenius type which is in accordance with determinations of the dynamics in the isotropic initial globule. The equilibration of the complete system, however, takes considerably longer than given by the diffusion on a length scale of the radius of gyration. The application of the simulated results to biopolymers was addressed.

- 
- [1] T. T. Perkins, S. R. Quake, D. E. Smith, and S. Chu, *Science* **264**, 822 (1994).  
 [2] T. T. Perkins, D. E. Smith, R. G. Larson, and S. Chu, *Science* **268**, 83 (1995).  
 [3] C. Bustamante, J. F. Marko, E. D. Siggia, and S. Smith, *Science* **265**, 1599 (1994).  
 [4] M. S. Z. Kellermayer, S. B. Smith, H. L. Granzier, and C. Bustamante, *Science* **276**, 1112 (1997).  
 [5] M. Rief, F. Oesterhelt, B. Heymann, and H. E. Gaub, *Science* **275**, 1295 (1997).  
 [6] L. Tskhovrebova, J. Trinick, J. A. Sleep, and R. M. Simmons, *Nature (London)* **387**, 308 (1997).  
 [7] P. Pincus, *Macromolecules* **9**, 386 (1976).  
 [8] I. Webman, J. L. Lebowitz, and M. H. Kalos, *Phys. Rev. A* **23**, 316 (1981).  
 [9] Y. Oono, T. Ohta, and K. F. Freed, *Macromolecules* **14**, 880 (1981).  
 [10] J. Gao and J. H. Weiner, *Macromolecules* **20**, 142 (1987).  
 [11] P. G. deGennes, *Scaling Concepts in Polymer Physics* (Cornell University Press, Ithaca, 1979).  
 [12] A. Yu. Grosberg and A. R. Khokhlov, *Statistical Physics of Macromolecules* (AIP, New York, 1994).  
 [13] M. Doi and S. F. Edwards, *The Theory of Polymer Dynamics* (Clarendon, Oxford, 1986).  
 [14] M. Wittkop, J.-U. Sommer, S. Kreitmeier, and D. Göritz, *Phys. Rev. E* **49**, 5472 (1994).  
 [15] S. Kreitmeier, M. Wittkop, and D. Göritz, *Macromol. Symp.* **100**, 181 (1995).  
 [16] C. Williams, F. Brochard, and H. L. Frisch, *Annu. Rev. Phys. Chem.* **32**, 433 (1981).

- [17] S. Kreitmeier and D. Göritz, *Makromol. Chem., Macromol. Symp.* **41**, 253 (1991).
- [18] D. Göritz, S. Kreitmeier, and M. Wittkop, *J. Macromol. Sci., Phys.* **B35**, 615 (1996).
- [19] A. Halperin and E. B. Zhulina, *Europhys. Lett.* **15**, 417 (1991); *Macromolecules* **24**, 5393 (1991).
- [20] P. Cifra and T. Bleha, *Macromol. Theory Simul.* **4**, 233 (1995).
- [21] P. Cifra and T. Bleha, *J. Chem. Soc., Faraday Trans.* **91**, 2465 (1995).
- [22] S. Kreitmeier, M. Wittkop, and D. Göritz, *J. Comput. Phys.* **112**, 267 (1994).
- [23] M. Wittkop, S. Kreitmeier, and D. Göritz, *Phys. Rev. E* **53**, 838 (1996).
- [24] M. Wittkop, S. Kreitmeier, and D. Göritz, *J. Chem. Soc., Faraday Trans.* **92**, 1375 (1996).
- [25] I. Carmesin and K. Kremer, *Macromolecules* **21**, 2819 (1988).
- [26] H. P. Deutsch and K. Binder, *J. Chem. Phys.* **94**, 2294 (1991).
- [27] W. Kuhn and F. Grün, *Kolloid-Z.* **101**, 248 (1942).
- [28] J. Baschnagel, K. Binder, W. Paul, M. Laso, U. W. Suter, I. Batoulis, W. Jilge, and T. Bürger, *J. Chem. Phys.* **95**, 6014 (1991).
- [29] J. Baschnagel, K. Qin, W. Paul, and K. Binder, *Macromolecules* **25**, 3117 (1992).
- [30] A. Kolinski, J. Skolnick, and R. Yaris, *J. Chem. Phys.* **85**, 3585 (1986).
- [31] M. Wittkop, S. Kreitmeier, and D. Göritz, *J. Chem. Phys.* **104**, 3373 (1996).
- [32] A. Milchev, W. Paul, and K. Binder, *J. Chem. Phys.* **99**, 4786 (1993).
- [33] P. G. De Gennes, *J. Phys. (France) Lett.* **46**, L639 (1985).